CRITICALLY SAMPLED GRAPH WAVELETS CONVERTED FROM LINEAR-PHASE BIORTHOGONAL WAVELETS

Akie Sakiyama and Yuichi Tanaka

Graduate School of BASE, Tokyo University of Agriculture and Technology
Koganei, Tokyo, 184-8588 Japan
Email: sakiyama@msp-lab.org, ytnk@cc.tuat.ac.jp

ABSTRACT

This paper presents a design method of critically sampled graph wavelet transforms (CSGWTs) utilizing real-valued biorthogonal linear-phase wavelets for regular signals. Their filter characteristics are equivalent to those of biorthogonal linear-phase wavelets and can be expressed by real-valued closed-form with the sum of sinusoidal waves in the graph spectral domain. The proposed CSGWTs satisfy the perfect reconstruction condition for graph signals. Since the proposed filters are smooth functions, they are well-behaved even if we use a lower-order polynomial approximation. The performance of the proposed CSGWTs is evaluated by comparison with existing CSGWTs.

Index Terms— Graph signal processing, graph wavelets, graph filter banks, discrete wavelet transform

1. INTRODUCTION

Graph signal processing has been a hot topic in signal and information processing for both theoretical and practical reasons [1–18]. From the theoretical viewpoint, there are close relationships among signal processing, information theory [19], (spectral) graph theory [20], and computational harmonic analysis [4, 21]. From the practical viewpoint, there is an extensive amount of data with irregular structures, e.g., sensor and brain networks [6, 10], traffic [8], learning [5, 22], and images [23–26].

The design of wavelets and filter banks is one of key issues in graph signal processing as well as regular signal processing. There are several kernels that form perfect reconstruction (PR) graph filter banks [4, 10, 12]. Although many of them are undecimated transforms, graph-based filter banks with downsampling operation have also been developed [2, 3, 15–17]. Since the downsampling effect of graph signals causes *spectral folding phenomenon*, which is similar to *aliasing* of regular signal processing, the filter banks are designed for bipartite graphs. The critically sampled graph wavelet transform (CSGWT) must satisfy the PR condition like that for regular signals.

The discrete wavelet transforms (DWTs) are very useful tools for regular signal processing [27–29]. One of widely known and commonly used DWTs is real-valued biorthogonal linear-phase PR wavelet transform (hereafter, "DWT"). Cohen-Daubechies-Feauveau (CDF) DWT [30] is highly effective in compression and its 9/7-tap and 5/3-tap versions are used in JPEG2000 standard [31].

In this paper, CSGWTs derived from the DWTs are proposed. In our recent paper [32], we proposed M-channel filter banks derived from real-valued linear-phase PR FIR filter banks. They are *undecimated* transforms, whereas this paper provides its extension, i.e., the graph wavelet filter banks with downsampling. We can easily obtain a wavelet transform having a desired characteristic in the graph spectral domain from the filter coefficients of the DWT. Their characteristics can be defined by real-valued closed-form expressions, so they are smooth functions. It is revealed that the CSGWTs derived from the DWTs also satisfy the PR condition for graph signals. We show design examples of the CSGWTs utilizing CDF DWTs. They are close to orthogonal and have high reconstruction SNRs even if we use a lower-order shifted Chebyshev polynomial approximation [4]. The performance of the proposed CSGWTs is validated in non-linear approximation experiments of signals on graphs.

The remaining of this paper is organized as follows. Preliminaries are summarized in the rest of this section. Section 2 gives the existing critically sampled wavelet transforms for graph signals and for regular signals. Section 3 presents the design method of the CSGWTs derived from the DWTs and clarifies that the proposed CSGWTs satisfy the PR condition for graph signals. The design examples and experimental results are shown in Section 4. Finally, Section 5 concludes the paper.

1.1. Preliminaries

A graph $\mathcal{G}$ is represented as $\mathcal{G} = \{\mathcal{V}, \mathcal{E}\}$, where $\mathcal{V}$ and $\mathcal{E}$ denote sets of nodes and edges, respectively. The graph signal is defined as $\boldsymbol{f} \in \mathbb{R}^N$. We will only consider a finite undirected graph with no loops or multiple edges. The number of nodes is $N = |\mathcal{V}|$, unless otherwise specified. The (m, n)-th element of the adjacency matrix $\mathbf{A}$ is the weight of the edge between m and n if m and n are connected, and 0 otherwise. The degree matrix $\mathbf{D}$ is a diagonal matrix and its m-th diagonal element is $d_{mm} = \sum_n a_{mn}$. The unnormalized graph Laplacian matrix (GLM) is defined as $\mathbf{L} := \mathbf{D} - \mathbf{A}$ and the symmetric normalized GLM is $\boldsymbol{\mathcal{L}} := \mathbf{D}^{-1/2}\mathbf{L}\mathbf{D}^{-1/2}$. The symmetric normalized GLM has the property that its eigenvalues are within the interval $[0, 2]$, and we will use $\boldsymbol{\mathcal{L}}$ in this paper. The eigenvalues of $\boldsymbol{\mathcal{L}}$ are λ_i and ordered as: $0 = \lambda_0 < \lambda_1 \leq \lambda_2 \ldots \leq \lambda_{N-1} \leq 2$ without loss of generality. The eigenvector $\boldsymbol{u}_{\lambda_i}$ corresponds to λ_i and satisfies $\boldsymbol{\mathcal{L}}\boldsymbol{u}_{\lambda_i} = \lambda_i \boldsymbol{u}_{\lambda_i}$. The entire spectrum of $\mathcal{G}$ is defined by $\sigma(\boldsymbol{\mathcal{L}}) := \{\lambda_0, \ldots, \lambda_{N-1}\}$. The projection matrix for the eigenspace V_{λ_i} is $\mathbf{P}_{\lambda_i} = \sum_{\lambda=\lambda_i} \boldsymbol{u}_\lambda \boldsymbol{u}_\lambda^T$ where $\boldsymbol{u}_\lambda^T$ is the transpose of $\boldsymbol{u}_\lambda$. Let $H(\lambda)$ be the spectral kernel of a filter $\mathbf{H}$ defined on the real line $\lambda \in [0, 2]$. The spectral domain filter can be written as

$$\mathbf{H} = H(\boldsymbol{\mathcal{L}}) = \sum_{\lambda \in \sigma(\boldsymbol{\mathcal{L}})} H(\lambda)\mathbf{P}_\lambda. \tag{1}$$

The graph spectral domain filtering can be simply denoted as $\mathbf{H}\boldsymbol{f}$.

This work was supported in part by MEXT Tenure-Track Promotion Program and MIC SCOPE Grant Number 142103007.

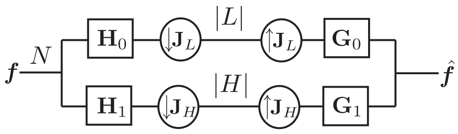

Fig. 1. Two-channel critically sampled graph wavelet transform.

2. CRITICALLY SAMPLED WAVELET TRANSFORMS

2.1. Two-Channel Wavelet Transforms for Graph Signals

A bipartite graph, whose nodes can be decomposed into two disjoint sets L and H such that every edge connects a node in L to one in H, can be represented as $\mathcal{G} = \{L, H, \mathcal{E}\}$. The downsampling function β_H of a bipartite graph is defined as $\beta_H(m) = +1$ if node $m \in H$ and $\beta_H(m) = -1$ if node $m \in L$. The diagonal downsampling matrix is $\mathbf{J}_H = \text{diag}\{\beta_H(m)\}$ and satisfies $\mathbf{J} = \mathbf{J}_H = -\mathbf{J}_L$. The downsampling-then-upsampling operation can be defined as follows:

$$\mathbf{D}_{du,L} = \frac{1}{2}(\mathbf{I}_N + \mathbf{J}_L),\ \mathbf{D}_{du,H} = \frac{1}{2}(\mathbf{I}_N + \mathbf{J}_H), \tag{2}$$

where $\mathbf{I}_N$ is an $N \times N$ identity matrix.

The CSGWTs decompose N input signals into $|L|$ lowpass coefficients and $|H|$ highpass coefficients, where $|L| + |H| = N$, as illustrated in Fig. 1. Since any arbitrary graph can be decomposed into K bipartite subgraphs, GWTs for bipartite graphs can be applied to any non-bipartite graphs [2, 33]. The PR condition of the CSGWTs can be expressed as

$$G_0(\lambda)H_0(\lambda) + G_1(\lambda)H_1(\lambda) = 2, \tag{3}$$
$$-G_0(\lambda)H_0(2-\lambda) + G_1(\lambda)H_1(2-\lambda) = 0. \tag{4}$$

Additionally, the orthogonal transform, graph-QMF [2], has the orthogonality condition $H_0^2(\lambda) + H_0^2(2-\lambda) = c^2$. The filters are chosen in a way that satisfies $H_1(\lambda) = H_0(2-\lambda)$, $H_0(\lambda) = G_0(\lambda)$ and $H_1(\lambda) = G_1(\lambda)$. Unfortunately, filters satisfying these conditions are not compact support. That is, if the graph-QMF were forced to be compact support, it would suffer from a loss of orthogonality and a reconstruction error. On the other hand, graphBior [3] relaxes the orthogonal condition of the graph-QMF. It satisfies the PR condition and has compact support because it uses an analogous approach to CDF construction for regular signals [30], i.e., it is based on the spectral factorizations of a maximally flat filter pair.

2.2. Two-Channel DWT for Regular Signals

In the z-domain, the PR condition of the two-channel DWT can be expressed as [28]

$$G_0(z)H_0(z) + G_1(z)H_1(z) = 2z^{-l}, \tag{5}$$
$$G_0(z)H_0(-z) + G_1(z)H_1(-z) = 0, \tag{6}$$

where $H_i(z) = \sum_{m=0}^{L_i-1} h_i(m)z^{-m}$, and L_0 and L_1 are the filter lengths of the lowpass filter $H_0(z)$ and the highpass filter $H_1(z)$, respectively. For aliasing cancellation, the synthesis filters are determined from analysis filters: $G_0(z) = H_1(-z)$ and $G_1(z) = -H_0(-z)$. For PR, (5) is rewritten as $P_0(z) - P_0(-z) = 2z^{-l}$ where $P_0(z) = G_0(z)H_0(z)$ and $l = \frac{L_0+L_1-2}{2}$. As a result, the design problem boils down to construct a half band filter $P(z) = z^l P_0(z)$ and obtain lowpass filters by spectral factorization of $P_0(z)$.

Proposition 1. *[34, Proposition 3.3], [28, Theorem 4.3] In two-channel biorthogonal linear-phase wavelet transforms, the filter lengths are all odd or all even. The analysis filters $H_0(z)$ and $H_1(z)$ should be*

a) Both symmetric of odd length, differing by an odd multiple of 2.

b) One symmetric and the other antisymmetric[1], of even length, and are equal or differ by an even multiple of 2.

3. CSGWT DERIVED FROM DWT

Wavelets in the graph spectral domain should be well-defined functions that cover the entire spectral range $\lambda \in [0, 2]$, and be real-valued functions. We used the discrete-time Fourier transform of the DWTs to construct the CSGWTs that have these properties.

3.1. Analysis Filters

In the frequency domain $\omega \in [0, \pi]$, the filter characteristics are formulated using the discrete-time Fourier transform. The transform is represented as $H_i(\omega) = \sum_{m=0}^{L_i-1} h_i(m)e^{-j\omega m}$. Because of symmetricity of filter coefficients, the frequency response of the analysis filters corresponding to the odd length DWT can be represented as the following form after elementary calculations:

$$H_i(\omega) = e^{-j\frac{L_i-1}{2}\omega}\left(2\sum_{m=0}^{(L_i-3)/2} h_i(m)\cos\left(\frac{b_{i,m}}{2}\omega\right) + h_i\left(\frac{L_i-1}{2}\right)\right), \tag{7}$$

where $b_{i,m} = L_i - (2m+1)$ and $i = 0, 1$. Similarly, the frequency response of the analysis filters corresponding to the even length DWT are

$$\begin{aligned} H_0(\omega) &= 2e^{-j\frac{L_0-1}{2}\omega}\sum_{m=0}^{(L_0-2)/2} h_0(m)\cos\left(\frac{b_{0,m}}{2}\omega\right), \\ H_1(\omega) &= 2je^{-j\frac{L_1-1}{2}\omega}\sum_{m=0}^{(L_1-2)/2} h_1(m)\sin\left(\frac{b_{1,m}}{2}\omega\right). \end{aligned} \tag{8}$$

From the above equations, the modulated frequency characteristics $\widehat{H}_i(\omega) = e^{j\frac{L_i-1}{2}\omega}H_i(\omega)$ become imaginary (for $H_1(\omega)$ of (8)) or real (otherwise) functions that cover $\omega \in [0, \pi]$.

By transforming the variables $\omega \in [0, \pi] \rightarrow \lambda \in [0, 2]$ and multiplying $\widehat{H}_1(\omega)$ of the even length DWT by $-j$, $\widehat{H}_i(\omega)$ becomes a real-valued function that covers the entire graph frequency range. As a result, the closed form of the analysis filters of the CSGWT derived from the odd length DWT are

$$H_i(\lambda) = 2\sum_{m=0}^{(L_i-3)/2} h_i(m)\cos\left(\frac{b_{i,m}\pi}{4}\lambda\right) + h_i\left(\frac{L_i-1}{2}\right), \tag{9}$$

and those derived from the even length DWT are

$$\begin{aligned} H_0(\lambda) &= 2\sum_{m=0}^{(L_0-2)/2} h_0(m)\cos\left(\frac{b_{0,m}\pi}{4}\lambda\right), \\ H_1(\lambda) &= 2\sum_{m=0}^{(L_1-2)/2} h_1(m)\sin\left(\frac{b_{1,m}\pi}{4}\lambda\right). \end{aligned} \tag{10}$$

[1]Generally, the lowpass filters is symmetric and highpass filters is anti-symmetric.

3.2. Synthesis Filters

In the z-domain, the synthesis filters of the DWT are expressed as

$$\begin{aligned} G_0(z) &= H_1(-z) = \sum_{m=0}^{L_1-1} (-1)^m h_1(m) z^{-m}, \\ G_1(z) &= -H_0(-z) = -\sum_{m=0}^{L_0-1} (-1)^m h_0(m) z^{-m}. \end{aligned} \tag{11}$$

The synthesis filters of the CSGWT derived from the odd length DWT are constructed by the same way as the analysis filters. They are represented as

$$\begin{aligned} &G_0(\lambda) = \\ &2\sum_{m=0}^{(L_1-3)/2} (-1)^m h_1(m) \cos\left(\frac{b_{1,m}\pi}{4}\lambda\right) + (-1)^{\frac{L_1-1}{2}} h_1\left(\frac{L_1-1}{2}\right), \\ &G_1(\lambda) = \\ &-2\sum_{m=0}^{(L_0-3)/2} (-1)^m h_0(m) \cos\left(\frac{b_{0,m}\pi}{4}\lambda\right) - (-1)^{\frac{L_0-1}{2}} h_0\left(\frac{L_0-1}{2}\right). \end{aligned} \tag{12}$$

The synthesis filters derived from the even length DWT are obtained by constructing $G_0(\lambda)$ and $G_1(\lambda)$ from a similar derivation as the analysis filters, and multiplying $G_1(\lambda)$ by -1. As a result, they are represented as

$$\begin{aligned} G_0(\lambda) &= 2\sum_{m=0}^{(L_1-2)/2} (-1)^m h_1(m) \cos\left(\frac{b_{1,m}\pi}{4}\lambda\right), \\ G_1(\lambda) &= 2\sum_{m=0}^{(L_0-2)/2} (-1)^m h_0(m) \sin\left(\frac{b_{0,m}\pi}{4}\lambda\right). \end{aligned} \tag{13}$$

Proposition 2. *The CSGWT derived from the DWT satisfies the PR condition in* (3) *and* (4).

Proof. Case 1: L_0 and L_1 are both odd. By multiplying both sides by $e^{j\frac{L_0+L_1-2}{2}\omega}$, (5) in the frequency domain $\omega \in [0, \pi]$ can be rewritten as

$$\widehat{G}_0(\omega)\widehat{H}_0(\omega) + \widehat{G}_1(\omega)\widehat{H}_1(\omega) = 2. \tag{14}$$

Then, the graph filters derived by transforming the variable $\omega \in [0, \pi] \to \lambda \in [0, 2]$ satisfy the following relationship:

$$G_0(\lambda)H_0(\lambda) + G_1(\lambda)H_1(\lambda) = 2. \tag{15}$$

The lowpass filter $G_0(\lambda)$ in (12) can be rewritten as

$$\begin{aligned} &G_0(\lambda) = \\ &(-1)^{\frac{L_1-1}{2}}\left(2\sum_{m=0}^{(L_1-3)/2} h_1(m) \cos\left(\frac{b_{1,m}\pi}{4}(2-\lambda)\right) + h_1\left(\frac{L_1-1}{2}\right)\right). \end{aligned}$$

Let us define $n_0, n_1 \in \mathbb{R}$. Here, $G_0(\lambda) = H_1(2-\lambda)$ for $L_1 = 4n_1+1$ and $G_0(\lambda) = -H_1(2-\lambda)$ for $L_1 = 4n_1+3$. With a similar derivation, it can be seen that $G_1(\lambda) = -H_0(2-\lambda)$ for $L_0 = 4n_0+1$ and $G_1(\lambda) = H_0(2-\lambda)$ for $L_0 = 4n_0+3$. From Proposition 1, the possible forms of the filter lengths are $\{L_0 = 4n_0+1, L_1 = 4n_1+3\}$, or $\{L_0 = 4n_0+3, L_1 = 4n_1+1\}$. In both cases, the CSGWT derived from the odd length DWT satisfies the PR condition in (3) and cancels the spectral folding phenomenon in (4).

Case 2: L_0 and L_1 are both even. Similar to the odd length case, (5) can be modulated as

$$\widehat{G}_0(\omega)\widehat{H}_0(\omega) + (j\widehat{G}_1(\omega))(-j\widehat{H}_1(\omega)) = 2. \tag{16}$$

Then, the graph filters satisfy

$$G_0(\lambda)H_0(\lambda) + G_1(\lambda)H_1(\lambda) = 2. \tag{17}$$

The synthesis filters in (12) are rewritten as

$$\begin{aligned} G_0(\lambda) &= 2\sum_{m=0}^{(L_1-2)/2} (-1)^{\frac{L_1-2}{2}} h_1(m) \sin\left(\frac{b_{1,m}\pi}{4}(2-\lambda)\right), \\ G_1(\lambda) &= 2\sum_{m=0}^{(L_0-2)/2} (-1)^{\frac{L_0-2}{2}} h_0(m) \cos\left(\frac{b_{0,m}\pi}{4}(2-\lambda)\right). \end{aligned} \tag{18}$$

It can be seen that the synthesis filters are $G_0(\lambda) = -H_1(2-\lambda)$ and $G_1(\lambda) = -H_0(2-\lambda)$ if $\{L_0 = 4n_0, L_1 = 4n_1\}$, or $G_0(\lambda) = H_1(2-\lambda)$ and $G_1(\lambda) = H_0(2-\lambda)$ if $\{L_0 = 4n_0+2, L_1 = 4n_1+2\}$. From the above, the CSGWT derived from the even length DWT also satisfies (3) and (4). □

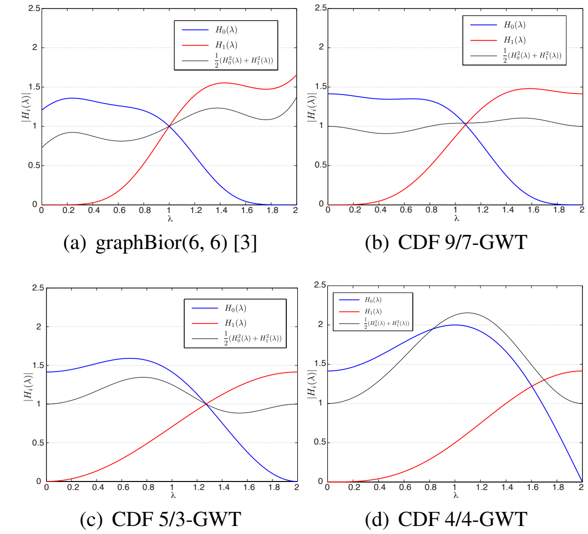

(a) graphBior(6, 6) [3] (b) CDF 9/7-GWT (c) CDF 5/3-GWT (d) CDF 4/4-GWT

Fig. 2. Analysis filters of CSGWTs. The black line indicates $\frac{1}{2}(H_0^2(\lambda) + H_1^2(\lambda))$.

Table 1. Performance Comparison (Average of 20 random bipartite graphs with $N = 500$): Orthogonality θ and reconstruction SNR (dB) with filter length p

p	graphQMF		graphBior		CDF 9/7-GWT		CDF 5/3-GWT	
	θ	SNR	θ	SNR	θ	SNR	θ	SNR
6	0.92	21.02	0.85	298.42	0.94	46.60	0.90	77.84
8	0.96	32.04	0.87	290.77	0.95	66.63	0.90	106.74
10	0.98	54.25	0.86	272.55	0.95	87.08	0.90	141.30
12	0.98	38.19	0.84	261.11	0.95	111.77	0.90	178.82
14	0.98	33.97	0.89	241.17	0.95	137.86	0.90	217.91
16	0.99	39.94	0.90	228.51	0.95	167.56	0.90	259.94
18	0.99	49.82	0.91	221.63	0.95	198.28	0.90	291.63
20	0.99	53.94	0.91	192.90	0.95	231.17	0.90	289.87

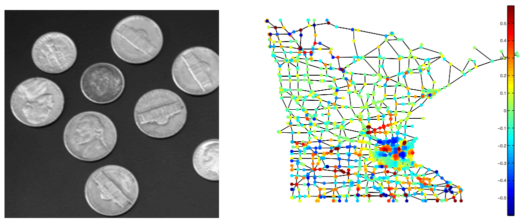

(a) *Coins* image (b) *Minnesota Traffic Graph*

Fig. 3. Input signals. We used the MATLAB code of Shuman et al. [12] for the signal on the *Minnesota Traffic Graph*.

4. DESIGN EXAMPLES AND EXPERIMENTAL RESULTS

4.1. Design Examples

Figure 2 shows examples of the CDF-based CSGWT (CDF-GWT). They are obtained by substituting the filter coefficients $h_i(m)$, $m = 0, 1, 2, \ldots, L_i - 1$ of the CDF DWTs [30] into (9) (for the CDF 9/7-GWT and the CDF 5/3-GWT) and (10) (for the CDF 4/4-GWT). For comparison, the frequency response of graphBior(6, 6) wavelet filter bank [3] is also shown. It can be seen the filter characteristics of the CDF-GWTs are equivalent to those of the CDF wavelets for regular signals.

4.2. Performance Comparison

If the spectral filter is a k degree polynomial, it is k-hop localized in the vertex domain [4] and does not require full eigendecomposition of a given normalized GLM $\boldsymbol{\mathcal{L}}$ for graph spectral filtering. Therefore, the p-th order Chebyshev polynomial approximation [4] is used for the graphQMF and the proposed CSGWTs.

The practical performance of the proposed CSGWTs are compared with the graphQMF (Meyer kernel) [2] and the graphBior [3]. The orthogonality and reconstruction error are summarized in Table 1. The orthogonality θ is defined as $\theta = 1 - \frac{|A-B|}{|A+B|}$ where $A = \sqrt{\inf_\lambda \frac{1}{2}(H_0^2(\lambda) + H_1^2(\lambda))}$ and $B = \sqrt{\sup_\lambda \frac{1}{2}(H_0^2(\lambda) + H_1^2(\lambda))}$ [3]. Because the filter kernels of the graphBior are defined by polynomials, the graphBior does not need the polynomial approximation and has high SNR (> 100dB) regardless of the filter lengths. However, its orthogonality is relatively low, especially for shorter filter lengths. The graphQMF is almost orthogonal, but its SNRs are very low even when $p = 20$ due to polynomial approximation. Although the polynomial approximation is also used for the CDF-GWTs, the CDF-GWTs can reproduce the ideal filter characteristics and show high orthogonality as well as high SNRs even with shorter filter lengths, since the CDF-GWTs covers the entire graph frequency range with one series of sinusoidal waves as shown in (9). It is worth noting that, in our approach, *any* biorthogonal linear-phase DWTs for regular signals are completely reusable for graph signals, and its filter characteristics in the graph spectral domain are easily estimated from its frequency domain counterpart.

4.3. Non-linear Approximation

The CDF 9/7 and 5/3-based CSGWTs are compared with the CDF 9/7 DWT for regular signals, the graphQMF [2], and the graphBior(5, 5) [3] in the non-linear approximation of image and graph signal. Figure 3 shows the original signals of *Coins* image and *Minnesota Traffic Graph*. All graph-based transforms are with filter length $p = 10$, and use edge-aware image graphs for *Coins* image [35]. After four-level (for *Coins* image) or one-level[2] (for the *Minnesota Traffic Graph*) decomposition, the input signal is reconstructed from all lowpass coefficients and some fraction of highpass coefficients. Figure 4 shows PSNR and SNR plotted against the fraction of highpass coefficients. In both signals, the proposed CSGWTs always outperform the other methods. Figure 5 shows the reconstructed *Coins* images. We can see that the CDF-GWTs suppress ringing artifacts compared to the other methods.

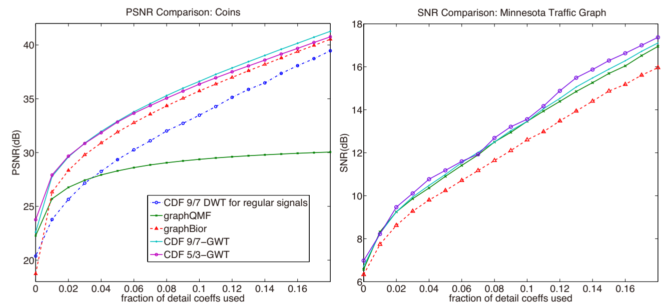

(a) *Coins* image (b) *Minnesota Traffic Graph*

Fig. 4. PSNR and SNR comparisons.

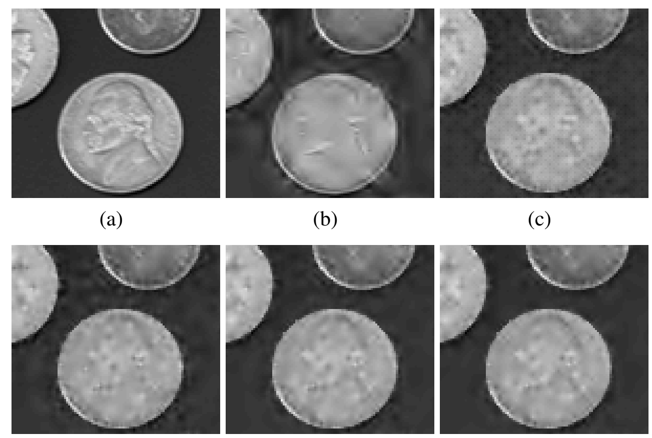

(a) (b) (c) (d) (e) (f)

Fig. 5. Zoomed in *Coins* images reconstructed from all lowpass coefficients and 3% of highpass coefficients. (a) Original image. (b) CDF 9/7 DWT(27.16dB). (c) graphQMF (27.92dB). (d) graphBior (29.79dB). (e) CDF 9/7-GWT (30.88dB). (f) CDF 5/3-GWT (30.85dB).

5. CONCLUSION

We proposed the CSGWTs derived from the DWTs for regular signals. The CSGWTs always satisfy the PR condition. They have high orthogonality and low reconstruction error even when we use lower-order Chebyshev approximations. They also outperform the existing CSGWTs in the non-linear approximation experiments.

[2]Since the edge-aware image graphs and *Minnesota Traffic Graph* are four-colorable and three-colorable graphs, respectively, they can be decomposed into two bipartite subgraphs and are applied two-dimensional CS-GWTs [2, 33].

6. REFERENCES

[1] D. I Shuman, S. K. Narang, P. Frossard, A. Ortega, and P. Vandergheynst, "The emerging field of signal processing on graphs: Extending high-dimensional data analysis to networks and other irregular domains," *IEEE Signal Process. Mag.*, vol. 30, no. 3, pp. 83–98, 2013.

[2] S. K. Narang and A. Ortega, "Perfect reconstruction two-channel wavelet filter banks for graph structured data," *IEEE Trans. Signal Process.*, vol. 60, no. 6, pp. 2786–2799, 2012.

[3] S. K. Narang and A. Ortega, "Compact support biorthogonal wavelet filterbanks for arbitrary undirected graphs," *IEEE Trans. Signal Process.*, vol. 61, no. 19, pp. 4673–4685, 2013.

[4] D. K. Hammond, P. Vandergheynst, and R. Gribonval, "Wavelets on graphs via spectral graph theory," *Applied and Computational Harmonic Analysis*, vol. 30, no. 2, pp. 129–150, 2011.

[5] M. Gavish, B. Nadler, and R. R. Coifman, "Multiscale wavelets on trees, graphs and high dimensional data: Theory and applications to semi supervised learning," in *Proc. ICML'10*, 2010, pp. 367–374.

[6] G. Shen and A. Ortega, "Transform-based distributed data gathering," *IEEE Trans. Signal Process.*, vol. 58, no. 7, pp. 3802–3815, 2010.

[7] W. Wang and K. Ramchandran, "Random multiresolution representations for arbitrary sensor network graphs," in *Proc. ICASSP'06*, 2006, pp. IV–161–IV–164.

[8] M. Crovella and E. Kolaczyk, "Graph wavelets for spatial traffic analysis," in *Proc. INFOCOM'03*, 2003, vol. 3, pp. 1848–1857.

[9] R. R. Coifman and M. Maggioni, "Diffusion wavelets," *Applied and Computational Harmonic Analysis*, vol. 21, no. 1, pp. 53–94, 2006.

[10] N. Leonardi and D. Van De Ville, "Tight wavelet frames on multislice graphs," *IEEE Trans. Signal Process.*, vol. 16, no. 13, pp. 3357–3367, 2013.

[11] C. Zhang and D. Florêncio, "Analyzing the optimality of predictive transform coding using graph-based models," *IEEE Signal Process. Lett.*, vol. 20, no. 1, pp. 106–109, 2012.

[12] D. I Shuman, C. Wiesmeyr, N. Holighaus, and P. Vandergheynst, "Spectrum-adapted tight graph wavelet and vertex-frequency frames," *arXiv preprint arXiv:1311.0897*, 2013.

[13] A. Sandryhaila and J. M. F. Moura, "Discrete signal processing on graphs," *IEEE Trans. Signal Process.*, vol. 61, no. 7, pp. 1644–1656, 2013.

[14] A. Sandryhaila and J. M. F. Moura, "Discrete signal processing on graphs: Frequency analysis," *IEEE Trans. Signal Process.*, vol. 62, no. 12, pp. 3042–3054, 2014.

[15] Y. Tanaka and A. Sakiyama, "M-channel oversampled graph filter banks," *IEEE Trans. Signal Process.*, vol. 62, pp. 3578–3590, 2014.

[16] Y. Tanaka and A. Sakiyama, "M-channel oversampled perfect reconstruction filter banks for graph signals," in *Proc. ICASSP'14*, 2014.

[17] A. Sakiyama and Y. Tanaka, "Oversampled graph Laplacian matrix for graph filter banks," *IEEE Trans. Signal Process.*, vol. 62, no. 24, pp. 6425–6437, Dec. 2014.

[18] Nathanaël Perraudin, Johan Paratte, David Shuman, Vassilis Kalofolias, Pierre Vandergheynst, and David K. Hammond, "Gspbox: A toolbox for signal processing on graphs," *ArXiv e-prints: arXiv:1408.5781*, Aug. 2014.

[19] A. Agaskar and Y. M. Lu, "A spectral graph uncertainty principle," *IEEE Trans. Inf. Theory*, vol. 59, no. 7, pp. 4338–4356, 2013.

[20] F. R. K. Chung, *Spectral Graph Theory (CBMS Regional Conference Series in Mathematics, No. 92)*, American Mathematical Society, 1997.

[21] D. I Shuman, B. Ricaud, and P. Vandergheynst, "Vertex-frequency analysis on graphs," *submitted to Applied and Computational Harmonic Analysis*, 2013.

[22] D. Thanou, D. I Shuman, and P. Frossard, "Parametric dictionary learning for graph signals," in *Proc. GlobalSIP'13*, 2013.

[23] F. Zhang and E. R. Hancock, "Graph spectral image smoothing using the heat kernel," *Pattern Recognition*, vol. 41, no. 11, pp. 3328–3342, 2008.

[24] A. Kheradmand and P. Milanfar, "A general framework for kernel similarity-based image denoising," in *Proc. GlobalSIP'13*, 2013, pp. 415–418.

[25] W. Hu, X. Li, G. Cheung, and O. Au, "Depth map denoising using graph-based transform and group sparsity," in *Proc. MMSP'13*, 2013.

[26] Y. Iizuka and Y. Tanaka, "Depth map denoising using collaborative graph wavelet shrinkage on connected image patches," in *Proc. ICIP'14*, 2014.

[27] M. Antonini, M. Barlaud, P. Mathieu, and I. Daubechies, "Image coding using wavelet transform," *IEEE Trans. Image Process.*, vol. 1, no. 2, pp. 205–220, 1992.

[28] G. Strang and T. Q. Nguyen, *Wavelets and Filter Banks*, Wellesley-Cambridge, MA, 1996.

[29] M. Vetterli and J. Kovačevic, *Wavelets and subband coding*, Prentice-Hall, NJ, 1995.

[30] A. Cohen, I. Daubechies, and J.-C. Feauveau, "Biorthogonal bases of compactly supported wavelets," *Communications on pure and applied mathematics*, vol. 45, no. 5, pp. 485–560, 1992.

[31] D. S. Taubman and M. W. Marcellin, *JPEG2000: Image Compression Fundamentals, Standards and Practice*, Kluwer, Norwell, MA, 2001.

[32] A. Sakiyama and Y. Tanaka, "On conversion of filter banks from the frequency domain to the graph spectral domain," *submitted to IEEE Trans. Signal Process.*, 2015.

[33] F. Harary, D. Hsu, and Z. Miller, "The biparticity of a graph," *J. Graph Theory*, vol. 1, no. 2, pp. 131–133, 1977.

[34] M. Vetterli and C. Herley, "Wavelets and filter banks: Theory and design," *IEEE Trans. Signal Process.*, vol. 40, no. 9, pp. 2207–2232, 1992.

[35] S. K. Narang, Y. H. Chao, and A. Ortega, "Graph-wavelet filterbanks for edge-aware image processing," in *Proc. IEEE SSP Workshop.*, pp. 141–144, Aug. 2012.